Research Paper

Whispering Gallery Mode Resonators at Optical and Terahertz Frequencies: A Brief Review

Arjun Rao[1*] , Cijy Mathai[2], Niraj Joshi[1], A. Jayarama[3], Siddartha Duttagupta[4]

A. V. Gopal[5], S. S. Prabhu[5] and Richard Pinto[1]

[1]E & C Dept.,Sahyadri College of Engineering & Management, Mangalore -575007

[2]Physics Dept., Indian Institute of Technology Bombay, Mumbai-400076

[3]Physics Dept., Sahyadri College of Engineering & Management, Mangalore -575007

[4]Electrical Engineering Dept., Indian Institute of Technology Bombay, Mumbai-400076

[5]Condensed Matter Physics and Material Sciences Dept., Tata Institute of Fundamental Research, Mumbai-400005

* Email: arjunsr92@gmail.com

Abstract

Whispering Gallery Mode Resonators represent a class of cavity devices with exceptional properties such as extremely small mode volume, very high power density, and very narrow spectral line width. Their importance for applications in very sensitive micro-sensors, have been recognized only in recent years. The sensitivity of this resonant technique has been found to be single molecular level, higher than that compared to most optical single-pass devices such as surface plasmon resonance biosensors. In this paper we present a brief review of the eld of WGM resonators, which includes the basic concept, the geometrical structures of resonators such as microdiscs, microtoroids and microspheres; the techniques for their fabrication and some of the most important applications as biosensors.

Keywords: WGMR, dielectric, THz, Optical, resonators, biosensor.

1 Introduction

Optical resonators play an important role in modern optics, both as optical lters as well as laser devices. They are also important for nonlinear optics experiments as well as accurate tools for measurements [1-5].

However, bulk optical resonators have certain limitations due to their weight, size, alignment and stability problems. Most of these problems have been overcome by the integrated optics approach. A particular class of resonators, which has emerged in the recent years and has found many applications, is that of integrated ring resonators [6].

In the spectrum of electromagnetic waves, the terahertz range is a narrow window with wavelengths between 3mm and 30m or frequencies between 100 GHz and 10 THz. The THz range, in between infrared and radio waves, has some unique properties. Most of the plastics, textiles, paper and cardboard etc., are transparent to terahertz waves. Further, many biomolecules such as proteins, narcotics and explosives, show characteristic absorption lines - spectral ngerprints - at terahertz frequencies. Further, terahertz waves do not cause any ionizing e ect and hence, are generally considered biologically safe. Figure 1 shows the spectrum of electromagnetic waves. Whispering gallery modes (WGM) are speci c resonant modes of a wave eld which are con ned inside a cavity with polished surfaces due to a series of total internal re ections. From practical considerations, the most interesting Whispering gallery mode resonators (WGMR) are in the optical domain, since they exhibit many unique properties, such as low mode volumes, small sizes of resonators and ultra-high Q-factors [7].

Historically, the phenomenon of whispering gallery waves was rst observed by Lord Rayleigh in the 19th century under the dome of St. Paul's cathedral in London. This phenomenon is due to the fact that while propagation of whiper or sound waves is directly proportional to the inverse of the square of the distance in normal mode, it is directly proportional to the inverse of the distance in whispering gallery mode. Subsequently, it was realized during the beginning of the 20th century that a phenomena similar to the acoustic whispering gallery waves could exist in the electromagnetic domain. However, the resonator dimensions required in the electromagnetic domain would be much smaller than those of the acoustic whispering gallery waves [7]. But the real study on WGMRs in the optical domain started only in 1990s. This lead to the study of WGMs in THz frequencies, which have an advantage of ease of fabrication of resonators and resonator coupling with the waveguides due to fact that the dimensions involved at THz frequencies are in the millimeter/sub millimeter range unlike the WGMRs in optical domain which are in micrometer range.

Further, the ease of fabrication and capability for on-chip integration of devices, makes WGMRs ideally suited for variety of applications. In this article, some key issues concerning WGMRs which include basic concept of WGMRs, simulation of WGMR at THz frequencies, resonator geometries, coupling of WGMRs with waveguides, resonator performance parameters and important practical applications are discussed.

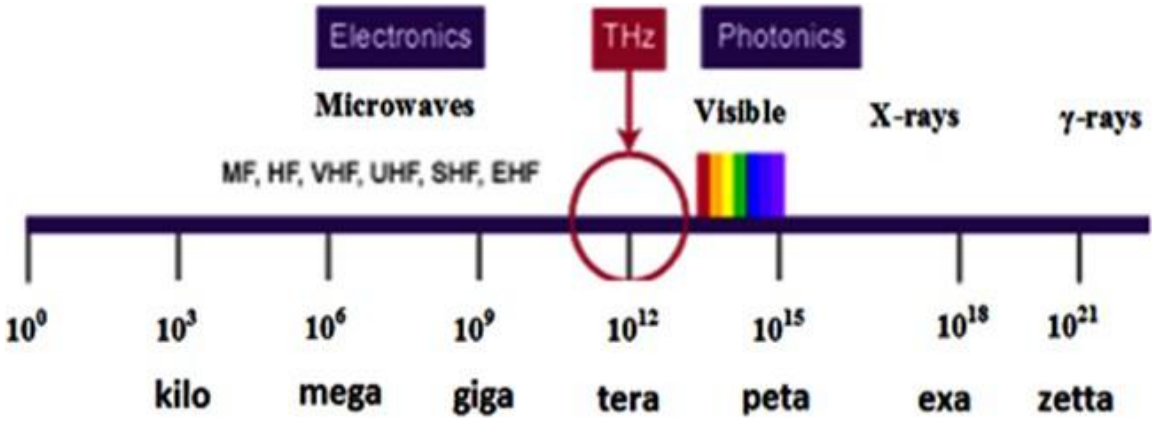

Figure 1: Spectrum of electromagnetic waves.

2 Whispering Gallery Mode Resonator

2.1 Basic Concept

Resonant phenomena in cavities in mechanical, acoustic and optical domains frequently depend on the geometric properties such as size and shape, and also on the composition of the cavities. Such resonances are often known as morphology-dependent resonances (MDRs). An important example of MDR is that of whispering gallery mode resonator in the acoustic domain [8]. As mentioned in the introduction, the WGM in the acoustic domain comprises a moving pressure wave guided around a closed concave surface, like the whispering gallery in St. Paul's Cathedral shown in a schematic Figure 2(a).

From geometric considerations, neglecting absorption, scattering, and material dispersion, these bound modes are guided by repeated total internal re ections and continue endlessly [8]. However, in reality, the wave losses continue through the surface via absorption, scattering, and material dispersion, and the mode undergoes a decay in its amplitude, in the absence of an external excitation [9], thereby causing a nite lifetime. It is important to note that WGM is a subclass of MDR and is characterized by its surface mode nature and high quality (Q) factors as a result of low losses.

Figure 2(b) shows the schematic of WGM in the optical domain illustrating WGMs can also occur in optical cavities having a closed concave interface. Among the most important and simplest WGM geometries in the optical domain are discs/cylinders, spheres, and ring cavities which have been studied extensively during the last two decades. Since the resonators in the optical domain are in the region of few 10's of micrometers, they are generally di cult to fabricate and also tune to the optical waveguide, though they give rise to extremely high Q factors. On the other hand, THz waves have an advantage since the WGMRs in the THz domain are in the sub-millimeter and millimeter range which are easy to fabricate and also to tune to the THz waveguide.

Hence, substantial work is going on currently on WGMRs in the THz domain.

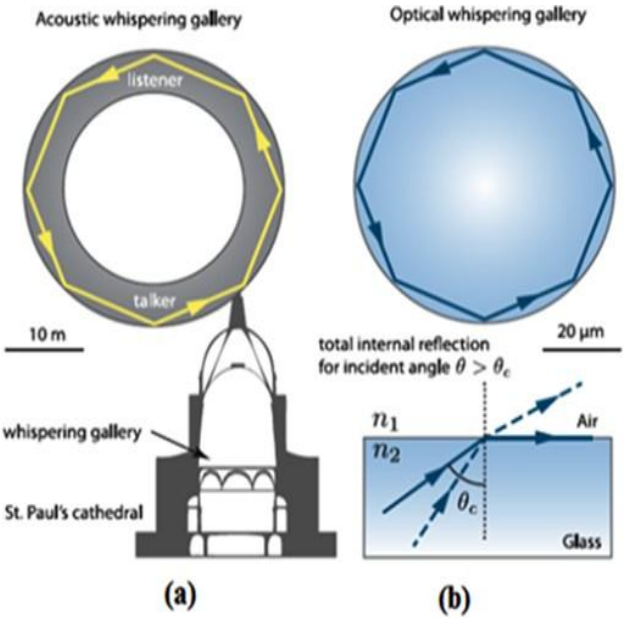

Figure 2: WGMs supported by total internal re ection in (a) an acoustic mode, and (b) an optical wave [10].

2.2 Simulation of WGMR tuned to a THz waveguide

An interesting phenomenon in optical as well as in THz domain for MGRs is that the continuous wave (CW) transmitted light intensity spectrum has several sharp peaks, depending upon the resonant conditions in WGMR, at very stable intervals between two successive peaks. The WGMR used in most cases is a low loss quartz microsphere in the case of optical domain and low loss quartz millimeter size microsphere in THz domain. Further, a minute change in the size of the microsphere or a change in the optical properties of the surrounding medium would shift resonant frequencies. In other words, molecular adsorption on the surface of the microsphere leads to a shift in resonant frequencies due to change in the e ective size of the microsphere and/or due to the change in the refractive index of the surrounding medium. Therefore, to detect a speci c molecule in extremely small

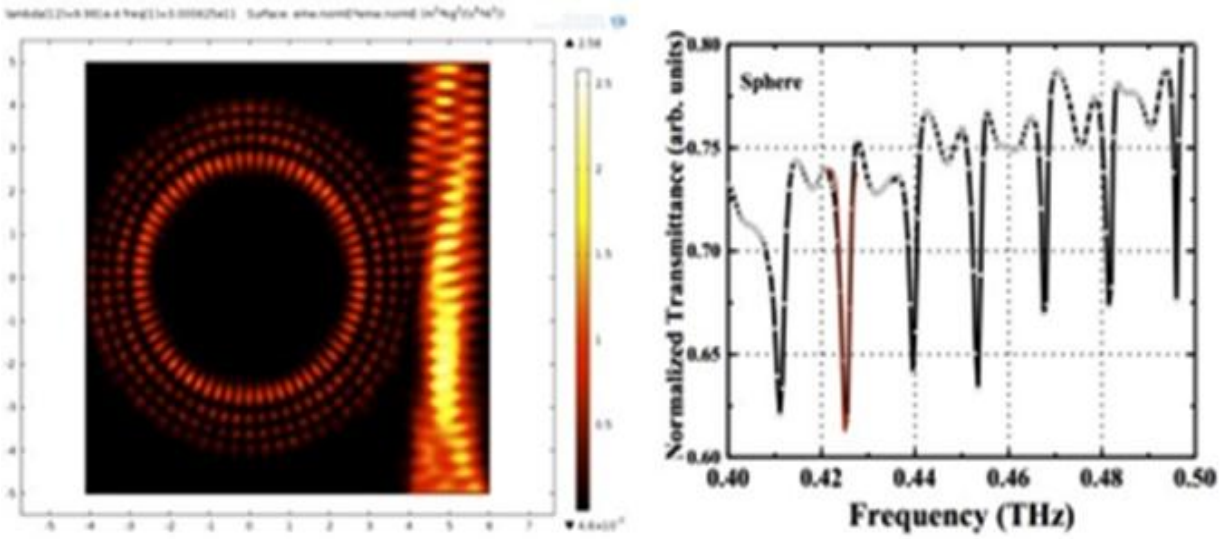

Figure 3: (a) WGMR response in the rectangular waveguide coupling mode. Cavity resonator material: Quartz (n=1.5), Dimension: 5 mm diameter. (b) Transmission spectrum of WGM cavity resonator. Also shown is the theoretical t Gaussian function for the resonance curve at 0.425 THz [11].

quantities, the WGMR con guration which includes the tunable range of excitation laser, the gap between the microsphere and waveguide, the microsphere size, and the refractive index of the materials, need to be designed and optimized. Since the experimental methods to optimize WGMR parameters are very involved and expensive, an approach to the problem with a simulation model is highly desirable [11].

Shown in Figure 3 is the simulation result obtained with 5 millimeter quartz sphere tuned to a rectangular THz waveguide in the CW-mode. Simulation was carried out using COMSOL Multiphysics vr. 4.4. Figure 3(a) shows WGMR response in the rectangular waveguide coupling mode. Cavity resonator material used is Quartz sphere with refractive index, n=1.5 and 5 mm diameter; Figure 3(b) shows the CW-transmission spectrum of WGM quartz cavity resonator, in which the red peak indicates a theoretical t Gaussian function for the resonance curve at 0.425 THz [11].

2.3 Quality factor of whispering gallery mode resonator

The most commonly used de nition of quality factor is frequency-to-bandwidth ratio of the resonator de ned as:

$$Q = \frac{f_r}{\Delta f} = \frac{\omega_r}{\Delta \omega} \quad (1)$$

where f_r is the resonant frequency, Δf is the resonance width or full width at half maximum; here, $\omega_r = 2\pi f_r$ is the angular resonant frequency and $\Delta\omega$ is the angular half-power bandwidth.

Most applications of WGMRs require the realization of very high Q factors. Since its rst demonstration in 1987, Q factor of microsphere WGMRs have improved from nearly 10^6 to 10^9 in the red and near-infrared areas of spectrum. It was realized that this Q factor was considerably lower than the limiting losses determined by intrinsic material qualities. It was also observed that in laboratory conditions the Q factor decreases within a short time span primarily due to deposition of micro dust and water vapour under high humidity conditions on the microsphere WGMR surface [12].

The Q factor of WGMR depends on four contributing factors as follows:

(a) Q_{rad} Q factor due to decay caused by the fact that, unlike a at surface, the total internal re ection from a curved surface leads to a radiation of the wave from the dielectric sphere. Such decay can be called the radiative decay. Corresponding to this phenomenon we de ne a radiative quality factor (Q_{rad}).

(b) Q_{ss} Quality factor due to surface scattering losses due to residual surface irregularities.

(c) Q_{Cont} Quality factor due to surface contamination.

(d) Q_{mat} Quality factor due to material property of the resonator; this is related to the contribution due to absorption of light and bulk Rayleigh scattering in the material of the microresonator.

Hence, e ective Q factor is

$$Q_{eff}^{-1} = Q_{rad}^{-1} + Q_{ss}^{-1} + Q_{cont}^{-1} + Q_{mat}^{-1} \quad (2)$$

where Q_{rad}^{-1} is due to intrinsic radiative (curvature) losses which vanish exponentially with increasing microsphere diameter D; so with $D/\lambda > 15$, $Q_{rad} > 10^{11}$ (λ is the wavelength); Q^{-1}_{ss} is due to scattering losses on residual surface irregularities which can prevail in intermediate sized microspheres. Q_{ss} can be calculated based on the model of Rayleigh scattering by molecular

sized surface inhomogeneities under grazing incidence and total internal re ection:

$$Q_{ss} = \frac{\lambda^2 D}{2\pi^2\sigma^2 B} \quad (3)$$

where σ and B are the rms roughness and the correlation length of surface irregularities, respectively. With the numerical values for σ = 0.3 nm and B = 3 nm reported for glass surfaces, one obtains $Q_{ss}^{-1} << 10^{-10}$ may be expected only in large spheres, D 100 μm.

Q_{Cont}^{-1} is due to losses introduced by surface contaminants. In the absence of contaminants the Q factor of large spheres would reach the limit obtained by material losses Q_{mat}^{-1} which is due intrinsic optical quality of the material of the microsphere. The principal limit for microsphere Q_{mat} is given by,

$$Q_{mat} = \frac{2\pi n}{\alpha\lambda} \quad (4)$$

where n is refractive index, α is attenuation coe cient and λ is wavelength. The measured Q in microspheres of high-purity fused silica with diameter 500 1000 μm fabricated by an oxygen hydrogen microburner at 633 nm is $\approx 0.9 \times 10^{10}$.

Further, larger Q ($\approx 10^{11}$) can be expected close to the minimum of attenuation at λ=1.55 μm wavelength in fused silica. In order to record Q values for applications it is important to not only fabricate high quality microspheres but also to preserve them in evacuated/dry gas lled chamber. Microspheres also can be preserved to achieve record Q factors by chemical treatment which prevents surface hydration from the atmosphere or by making the surface hydrophobic.

3 WGMR at THz frequencies

3.1 Coupling methods

WGM microsphere cavities are intrinsically high quality resonators and one of the important considerations for applications is the e ciency of light evanescent coupling with the waveguide. Figure 4 shows a schematic of a spherical WGM resonator and the waveguide.

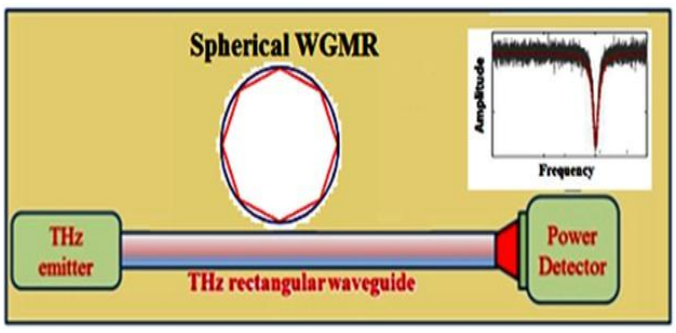

Figure 4: Schematic of a spherical WGM resonator coupled to waveguide (direct waveguide coupling).

WGM optical coupling using propagative free beams is not e cient due to the weak radiative transfer to WGMs which can be seen as quasi-bound state of light trapped inside a dielectric material. Many methods have been developed to overcome this disadvantage. They all rely on energy exchange between a WGM and total internal re ection waves or the evanescent part of guided modes. The prism coupling con guration described in Figure 5(a), based on total internal re ection, is the earliest method used to couple light in WGM microresonators [13-15]. This approach can be implemented using an angle polished optical ber instead of a prism [16] as shown in Figure 5(b). More recently, tapered bers have been used to critically couple microsphere high-Q-factor WGM resonators [17-19] as shown in see Figure 5(c).

Using this technique, it is possible to obtain transfer of the incoming power to the microresonator mode [17]. In integrated optics, optical waveguides are used to e ciently couple light inside WGM discs or microspheres [20-22]. The coupling e ciency can be adjusted by controlling the gap between the optical waveguide and the resonator.

3.2 Measurement methods

Primarily two types of measurement techniques can be used to accurately measure high-Q-factor of WGM resonators based on the analysis of the intensity transmission transient pro le namely, stationary approach and dynamical approach.

Stationary approach: The most common method used to measure the Q-factors of high and ultra-high-quality WGM microresonators involves linearly scanning of the frequency of a narrow probe laser at the input of the resonator and to simultaneously record its transmission as shown in Figure 4. The frequency of the laser is linearly swept while keeping the amplitude |sin(t)| constant. The source is modeled by as a monochromatic signal whose instantaneous frequency is written as $\nu(t) = \nu_i + \nu_s(t)$, where ν_i is the initial frequency and ν_i is the frequency sweeping rate. The laser probe is attenuated only when it is tuned to the resonator frequency ν_0 (resonant frequency). Experimentally, one can observe, in the time domain, a dip in the transmission spectrum of the resonator as shown in Figure 4. An accurate calibration of ν_s allows the frequency spectrum to be measured [12].

Dynamical approach: The Stationary approach is valid only for very low sweeping rates, $\nu_s << \nu_{so}$, which is necessary to record the stationary response of the resonator; ν_{so} is the scanning rate corresponding to bandwidth of the resonator. For higher-frequency sweeping rates, the excitation cannot be considered as stationary and a ringing phenomenon strongly modi es the pro le of the transmission spectrum due to the beating of the input and the intracavity elds [22-24].

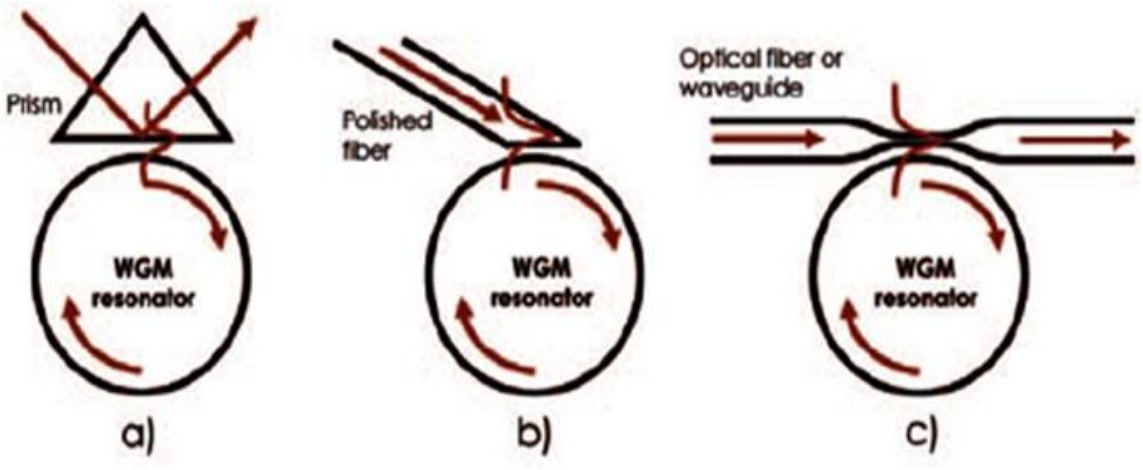

Figure 5: a) Prism coupling using frustrated total internal re ection (kretschmann geometry); b) Slant-cut optical ber coupling; c) Tapered ber or optical waveguide coupling [12].

4 Fabrication of WGM micro resonators

As described in above sections, there are many geometries of WGMRs, each of them having advantages and drawbacks. Three major parameters that must be considered in order to assess the usefulness of a given type are: the optical quality of the resonator material, the ease of fabrication and the achievable value of Q-factor. The fabrication techniques of the most common resonating structures are reviewed in this section [12]. Among the resonator materials, glasses, and in particular high purity optical grade silica, are widely used primarily because of the di culty in fabrication and also the high cost of crystalline materials. Several WGM resonators have been fabricated in the form of ring, sphere, toroid, and elliptical geometries which have been implemented using a wide variety of materials, including glass, silicon, compound semiconductors, silica, and crystalline material. Many methods have been used to fabricate WGMRs with standard semiconductor processing techniques. Ferroelectric resonators can also be used for engineering of the modal spectrum with RF and applied DC elds, since refraction index of the ferroelectric material changes with applied electrical eld [12]. It is also interesting to note that, calcium uoride and magnesium uoride resonators made with highly transparent crystals, exhibit the highest reported Q factors. A brief review of fabrication methods and the Q factors obtained with cylindrical, disc, toroidal and microspherical WGMRs is presented below.

4.1 Cylindrical

Cylindrical WGMRs have the simplest geometry and are easy to fabricate. However, they have the drawback that, due to the longitudinal degree of freedom in such a structure, a coupled beam in this case, as compared to the microsphere, spreads along the cylinder length and eventually vanishes. This happens even if there is no material loss [12]. One of the earliest experiments designed to show, that spiral whispering mode propagation occurs in closed optical structures of circular cross section, was carried out using cylinders machined from polymethyl methacrylate [25]. The simplest cylindrical WGMR, however, is fabricated with a small piece of a conventional telecom single-mode optical ber (chosen due to its high material quality), prepared by suitably stripping the cladding and coating [26, 27]. In this case, too, an experimental analysis has shown that if the ber is tilted i.e. not exactly perpendicular to the in-coupled optical beam, then spiral WGMs, tracing a helical path along the ber, are triggered. Hence, WGMR cylindrical geometries are generally not preferred [28].

4.2 Microdiscs and Toroids

Some of the early solid-state lasers were among the rst devices e ectively exploiting WGM light con nement [29, 30]. Walsh (1963) et al., have reported pulsed laser operation at room temperature by exploiting total internal re ection in a ruby ring. One of their ring lasers had internal diameter 22.2 mm, external diameter 23.8 mm, and height 3.18 mm; the other one 14.3 mm 15.9 mm, and 3.2 mm respectively. The c-axis was perpendicular to the plane of both rings, and concentration was 0.05% by weight. The rings were fabricated and mechanically polished; all surfaces except the inside diameter surface were optically polished. The authors estimated that the Q-value of these cavities was between 10^8 and 10^9, and noted that these values were about two orders of magnitude larger than those measured in silvered rods [30]. In the same year, Ross et. al. fabricated two lasers in cylindrical toroids of ruby, the material being a 0.035% ruby of medium quality, with c-axis oriented at 90° to toroid axis. The size of these compact lasers was 13mm outer diameter, 9mm or 11mm inner diameter, 5mm height. They reported the outstanding property of this approach which made it possible to combine an extremely high resonator Q with a moderate mode selection which led to quasi-continuous oscillations in an inhomogeneous material like ruby [29].

All these millimeter-sized resonators were produced by

mechanical polishing followed by thermal annealing. The JPL group [31], has developed a fabrication technique which is based on computer controled precision lathe, followed by a conventional polishing technique. By using the diamond turning process they were also able to realize a special single-mode cavity, formed by a small 5 μm x 3 μm waveguide on top of a cylinder [32].

In a very recent paper [33], a similar procedure was used to fabricate high-Q lithium niobate discs and spheroids made from Z-cut lithium niobate wafers. The polishing procedure of crystalline discs was in this case optimized by using a lapping machine. The almost spherical pro le was obtained through a rotational stage whose pivot point could be nely adjusted followed by elaborate polishing and cleaning steps. In this way they achieved an intrinsic disc Q-factor of 1.3×10^8.

Both microdiscs and microspheres by virtue of their being discrete objects make them di cult to be coupled to optical integrated circuits. Further, optical polishing cannot be easily adapted to sub-mm devices. In this context, for the development of micron-sized robust integrated devices a much more e ective approach is the one rst proposed by Vahala's group [34] who demonstrated a method for fabricating toroid-shaped silica microresonators-on-a-chip with Q values in excess of 10^8. Figure 6 shows a scanning electron micrograph of a silica microdisc, fabricated on silicon wafers prepared with a 2 μm layer of silicon dioxide.

Figure 6: SEM image of a silica microdisc [36].

The fabrication process for the torroid microresonator composed of four steps as follows: photolithography to create disc-shaped photo-resist pads typically 160 μm diameter; pattern transfer into the SiO_2 layer; selective dry etch followed by selective re ow of the patterned silica. They demonstrated a chip-based monolithic microcavity Raman laser, exhibiting high e ciency, ultralow threshold, and single-mode emission. For a microtoroid with diameter $\approx$ 61μm and thickness $\approx$ 3.7μm they measured a quality factor and a threshold power at 1550 nm $\approx$ 74 μW for Raman lasing near 1680nm [35].

In another experiment, stimulated emission was achieved by incorporating erbium ions into the toroidal microcavity; this was realised by a group in Grenoble [37], that developed a process for the integration of silicon-rich oxide (SRO) layers doped with Er into toroidal microcavities. The SRO:Er thin lm was obtained in a high vacuum vessel by coevaporation under N atmosphere of silicon monoxide and erbium. Each sample was annealed under forming gas (95% - 5%) to activate emitters. First, silica microdiscs on circular silicon pillars were fabricated by de ning the discs in photoresist by optical lithography and transferring them to the silica or SRO layer by chemical etching using bu ered HF; arrays of silica microdiscs on silicon pillars were obtained by etching the silicon substrate by SF_6/Ar reactive ion etching. In a second step, CO_2 laser was used for selective re ow treatment to form the toroidal microcavities, by taking advantage of the much larger (100:1) thermal conductivity of silicon than silica. During re ow treatment, only the silica layer is heated, cooling the centre of the silica microdisc and the silicon pillar acts as a heat-sink. This results in a selective melting and smoothing of the edge of the silica disc, without a ecting its centre. It was noted that the nal surface roughness of a toroidal microcavity produced is close to that of a liquid droplet, as can be seen in the micrograph of Figure 7.

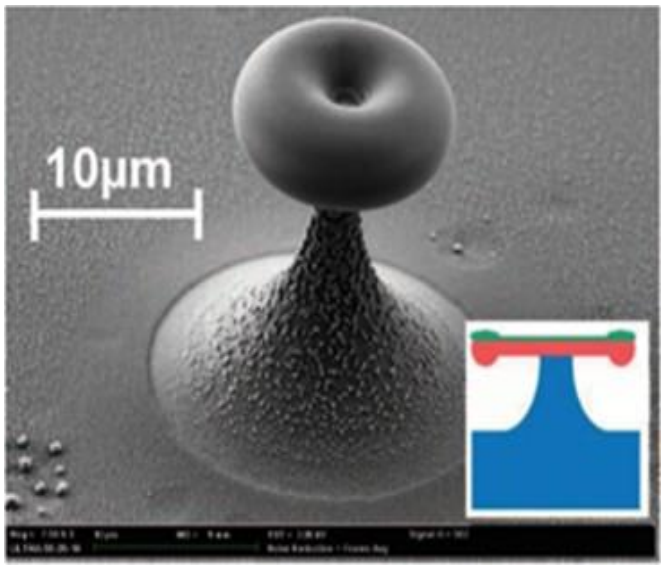

Figure 7: Scanning electron micrograph of a toroidal microresonator of diameter 13 μm after selective re ow. An SRO:Er layer 200nm thick had previously been deposited on top of a 2.7 μm silica layer [37].

4.3 Spherical

One of the main important advantages of microspheres is that they can be fabricated in the laboratory from a variety of inorganic and organic materials. Liquid microdroplets or microspheres have been studied since the very beginning of this eld. In recent years, polymer microspheres and their dispersions have been widely used in photonics as well as in medical and biochemical applications [38]. Polymer microspheres can be fabricated both by chemical methods such as heterogeneous polymerization and by physical methods, like emulsi cation, coacervation and spray-drying [12]. One important route is to fabricate rst a PMMA ber

followed by fabrication of a microsphere by melting the tip of the ber, just as in the case of silica microspheres. The Q-factor of the microspheres was found to be rather low ($\approx 5 \times 10^4$) [39], most likely due to impurities in the material and surface inhomogeneities caused by uneven heating. Later, the same authors [39], improved the Q-factor up to 10^6 by removing the impurities in the polymer. Microspheres were prepared by placing a controlled drop of the puri ed PMMA using a microsyringe at the tip of a PMMA ber. Hollow PMMA spheres could also be obtained by injecting a certain amount of air into the liquid polymer before depositing it onto the ber tip. Using another approach Li et al.[40], fabricated dye molecule-doped microspheres in a micro uidic channel, which can also create arrays onto a chip.

Fabrication of glass microspheres can be carried out using variety of techniques. One technique is based on the melting of glass powder in the furnace and dropping the viscous glass onto a spinning plate [12]. A process, used for a multi-component uoride glass (ZrF_4) is based on melting the raw materials at 1000°C inside an induction furnace; the molten material is poured in a ne stream into liquid N_2 followed by collection of spherical particles which passed through a lter [41]. One problem in this technique is the easy contamination of the sphere surface. Hence, chemical polishing in chemicals like $ZrOCl_2$ $8H_2O$ is required. Another approach involves the use of magnetic levitation to keep the glass sample suspended while heated. Here, a glass cube, located in a platinum cage at the edge of the inner magnet, is made to levitate while melting by the e ect of a focused CO_2 laser beam; glass microspheres were obtained after cooling [42, 43]. Subsequent polishing to optical grade improves the quality of the spheres. Another method to produce glass microspheres made use of a rotating electric arc. Microspheres with diameters between 2 and 24 μm were fabricated by processing of the glass powder; 85% of particles were transformed into microspheres [44]. One disadvantage of these techniques is however, is that one obtains a number of free spheres with a rather large size distribution which are di cult to be controlled [12]. The selected spheres can be picked up with an evacuated glass capillary for further use as a WGMR.

Another simple and e ective method to produce micro spheres with the desired diameter is based on the melting of the tip of a glass ber using di erent heating sources, such as high-power CO_2 laser and electric arc etc. [45, 46]. With heating the distal tip of a ber, the glass re ows to form a spherical volume due to surface tension. Because of high viscosity of silica, the re owed structure becomes highly spherical and extremely uniform with eccentricities as low as 1 2%. Further, the spherical surface has low intrinsic roughness, as low as 1 nm r.m.s, thereby causing very small surface scattering losses. A typical silica microsphere obtained in this way is shown in Figure 8(b). The light coupling in the tapered ber can be seen in the background (out of focus). The operation of the resonator is not a ected by the presence of the stem due to negligible overlap with the perturbation region, since the excited optical modes typically lie in the equatorial plane; on the other hand, it helps easy handling of the microsphere. Reproducible spherical diameters were obtained with the size of the spheres increasing with increasing number of electric arc shots, till the diameter saturated at about 350 m in the case of standard 125 μm singlemode optical bers. Figure 8(a) shows the growth of the sphere diameter with the number of shots; the picture of a typical 250 μm microsphere is shown in gure 8(b). This technique allows one to fabricate microspheres with diameters in the range d to 2d, where d is the outer diameter of the uncoated ber. Spheres, from 20 to 100 μm range can be obtained by tapering the ber. The minimum diameter obtained was 40 μm using tapered bers [47].

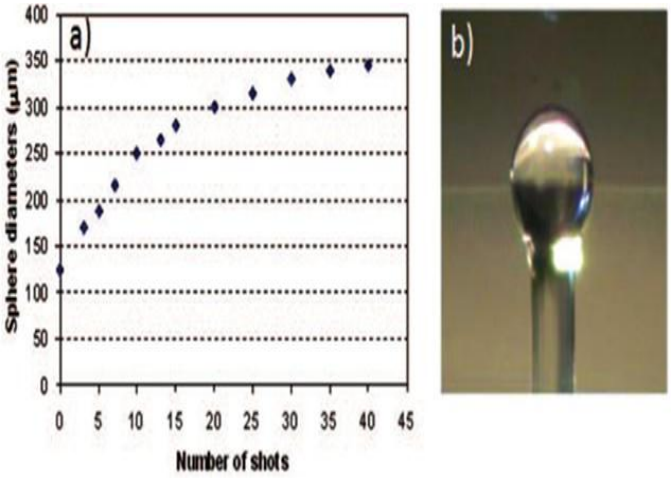

Figure 8: a) Size of the microspheres prepared at the tip of a 125 μm telecom ber, as a function of the arc shots. b) Optical image of a microsphere with 250 μm diameter [47].

5 Applications

WGMRs exhibit unique properties in the eld of sensing. The main advantage of a WGMR sensor is due to the fact that, the trapped photons are able to circulate on their orbit several times before exiting the WGMR if scattering losses by total internal re ection at the boundary of the resonator are low and absorption of light in the material is extremely low. In this section we present one particular eld of sensor applications viz biosensing by microspherical WGMRs, where rapid progress has been achieved during the last few years.

The sensing mechanism is based on the fact that, when a nano or microscopic object (like a molecule or a bacterium) is brought in proximity with the con ned circulating light, the interaction is resonantly reinforced due to the reactive mechanism. A change in the Q-factor of the WGMR or a shift in the resonance frequency is caused due to the change in radius and/or refractive index of the surface of the sphere, through the interaction of the evanescent part of the WGM eld. In principle, the sensitivity can be very high such that it can detect single molecules or single nanoparticles.

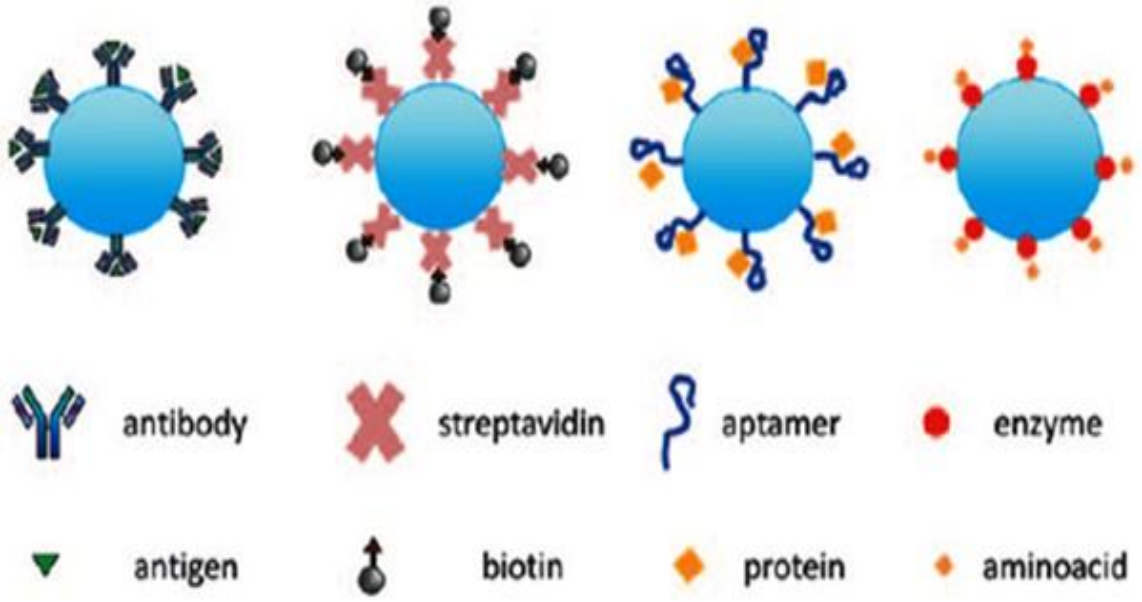

Figure 9: Schematic of a WGM biosensor, resulting from the combination of a WGMR with a sensing layer. Middle row: main ligands or receptors. Bottom: main analytes [12].

The characteristics of a WGM miniature biosensor based on ber-microsphere coupling have been studied numerically [48]. The authors have solved time-domain Maxwell's equations to obtain electromagnetic and radiation elds. They found a down-shift in the microsphere WGM resonance frequency due to an increase of either the refractive index of the surrounding medium or the e ective microsphere size. The larger the change, the stronger the shift is. They also found a linear relationship between e ective diameter of the microsphere and the resonance frequency shift.

It has been estimated by simulation [49] that for an optical instrument with ≈1 MHz resolution, a sensitivity of the WGMR biosensor as good as≈ 0.1 nm for the detection of attachment/adsorption of molecules on the microsphere and as good as $\approx 10^{-3}$ for the detection of refractive index change in the surrounding medium is achievable. Such high sensitivities of WGM miniature biosensors are extremely important in applications such as drug discovery, protein identi cation, peptide monitoring, DNA detection, etc. The important characteristics of a WGMR based biosensor are sensitivity, selectivity, reversibility and stability. The biochemical receptors such as antibody, antigen, DNA, enzyme and aptamer mainly provide for the selectivity as well as stability and reversibility of the WGM biosensor. The sensitivity is primarily being provided by the quality of the optical platform.

A schematic of a biosensor based on WGM resonators, after the functionalization, interfaced with the biological recognition element is shown in Figure 9. A schematic of the generally used biological recognition elements: antibody, streptavidin, aptamer and enzyme is shown in middle row in Figure 9; the bottom row in Figure 9 shows the corresponding analytes: antigen, biotin, proteins, and amino acids. The sensors based on antibody are known as immunosensors while aptamer-based sensors are called aptasensors. The antibody shows high speci city and a nity towards the antigen, as indicated by their molecular complementarities. Enzymes are speci c in both the substrate they recognize and the reaction they catalyze; Their activities are also regulated by other molecules.

The rst experiment that showed the quantitative use of spherical WGMR microsensors in biomedicine dates back to 2002 [50]. Speci c detection of proteins was proven in this paper. Further, the same group demonstrated single nucleotide polymorphism analysis by hybridization and the feasibility of multiplexed DNA quanti cation. An unprecedented sensitivity of 6 pg/mm^2 was demonstrated. By using two microspheres, speci c and multiplexed DNA detection was performed, leading to discriminate a single nucleotide mismatch. This technique can be of immense use in detection of gene mutation involved in cancer growth without target labeling.

6 Summary

Light Con nement into small volumes has become an essential requirement for photonic devices. Examples of this are integrated optical circuits, optical bers, and semiconductor lasers. Whispering Gallery Mode Resonators represent another class of cavity devices with exceptional properties such as very high power density, extremely small mode volume, and very narrow spectral line width. Optical dielectric resonators based on WGMRs are now known since more than three decades. However, their importance for applications in very sensitive microsensors, have been recognized only in recent years. A brief review of the eld of WGM resonators, which includes basic concept, the geometrical structures of resonators such as microdiscs, microtoroids

and microspheres; the techniques for their fabrication and some of the most important applications as biosensors are described here.

References

[1]D. Hall and P. Jackson, The Physics and Technology of Laser Resonators , Taylor and Francis, 1989.

[2]V. Bykov and O. Silichev, Laser Resonators , Cambridge Intl. Science Publ., 1995.

[3]A. Kudryashov and H. Weber, Laser Resonators: Novel Design and Development , SPIE Press, 1999.

[4]N. Hodgson and H. Weber, Laser Resonators and Beam Propagation, 2nd edition , Springer, 2005.

[5]S. K. Dixit, Filtering Resonators , Nova Science Publishers, 2001.

[6]D. G. Rabus, Integrated Ring Resonators: The Compendium , Springer, 2007.

[7]Matja^{o} Gomil²ek, Whispering gallery modes , Ljubljana, Seminar Report, November 2011.

[8]R. Matthew Foreman, D. Jon Swaim and Frank Vollmer, Whispering gallery mode sensors , Max Planck Institute for the Science of Light, Germany, May 2015.

[9]B. R. Johnson, Theory of morphology-dependent resonances: shape resonances and width formulas, J. Opt. Soc. Am. A, vol. 10, pp. 343 352, 1993.

[10]F. Vollmer and S. Roy, Optical resonator based biomolecular sensors and logic devices, J. Indian Inst. Sci., vol. 92, pp. 233 251, 2012.

[11]C. Mathai, S. Prabhu, A. Venugopal, N. Joshi, R. Pinto and S. P. Duttagupta, Tunable whispering gallery mode cavity in THz frequency domain for sensing applications , unpublished.

[12]G. C. Righini, Y.Dumeige, P. F'eron, M. Ferrari, G. Nunzi Conti, D. Ristic and S. Soria, Whispering gallery mode microresonators: Fundamentals and applications , vol. 34, 2011.

[13]V. Braginsky, M. Gorodetsky and V. Ilchenko, Phys. Lett. A, vol. 137, pp. 393, 1989.

[14]M. L. Gorodetsky and V. S. Ilchenko, J. Opt. Soc. Am. B, vol. 16, pp. 147, 1999.

[15]F. Treussart, V. Ilchenko, J. Roch, J. Hare, V. Lef`evre-Seguin, J. M. Raimond and S. Haroche, Eur. Phys. J. D, vol. 1, pp. 235, 1998.

[16]V. S. Ilchenko, X. S. Yao and L. Maleki, Opt. Lett., vol. 24, pp. 723, 1999.

[17]M. Cai, O. Painter and K. Vahala, Phys. Rev. Lett., vol. 85, pp. 74, 2000.

[18]V. S. Ilchenko, X. S. Yao and L. Maleki, Opt. Lett., vol. 24, pp. 723, 1999.

[19]J. C. Knight, G. Cheung, F. Jacques and T. A. Birks, Opt. Lett., vol. 22, pp. 1129, 1997.

[20]Y. Panitchob, G. S. Murugan, M. N. Zervas, P. Horak, S. Berneschi, S. Pelli, G. Nunzi Conti and J. S. Wilkinson, Opt. Express, vol. 16, pp. 11066, 2008.

[21]G. Nunzi Conti, S. Berneschi, F. Cosi, S. Pelli, S. Soria, G. C. Righini, M. Dispenza and A. Secchi, Opt. Express, vol. 19, pp. 3651, 2011.

[22]A. A. Savchenkov, A. B. Matsko, V. S. Ilchenko and L. Maleki, Opt. Express, vol. 15, pp. 6768, 2007.

[23]Z. Ioannidis, P. Radmore and I. Giles, Opt. Lett., vol. 13, pp. 422, 1988.

[24]J. Poirson, F. Bretenaker, M. Vallet and A. L. Floch, J. Opt. Soc. Am. B, vol. 14, pp. 2811, 1997.

[25]F. G. Reick, Appl. Opt., vol. 4, pp. 1396, 1965.

[26]T. A. Birks, J. C. Knight and T. E. Dimmick, IEEE Phot. Techn. Lett., vol. 12, pp. 182, 2000.

[27]M. Sumetsky and Y. Dulashko, OSA Proc. OFC-2006, 2006.

[28]A. W. Poon, R. K. Chang and J. A. Lock, Opt. Lett., vol. 23, pp. 1105, 1998.

[29]D. Ross, Proc. IEEE, vol. 51, pp. 468, 1963.

[30]P. Walsh and G. Kemeny, J. Appl. Phys., vol. 34, pp. 956, 1963.

[31]I. S. Grudinin and L. Maleki, Opt. Lett., vol. 32, pp. 166, 2007.

[32]I. Grudinin and L. Maleki, J. Opt. Soc. Am. B, vol. 25, pp. 594, 2008.

[33]G. Nunzi Conti, S. Berneschi, F. Cosi, S. Pelli, S. Soria, G. C. Righini and M. Dispenza, Opt. Express, vol. 19, pp. 3651, 2011.

[34]D. K. Armani, T. J. Kippenberg, S. M. Spillane and K. J. Vahala, Nature, vol. 421, pp. 925, 2003.

[35]T. Kippenberg, S. Spillane, D. Armani and K. J. V., Opt. Lett., vol. 29, pp. 1224, 2004.

[36]D. K. Armani, T. J. Kippenberg, S. M. Spillane and K. J. Vahala, Nature, vol. 421, pp. 925, 2003.

[37]J. B. Jager, P. Noe, E. Picard, V. Calvo, E. Delamadeleine and E. Hadji, Physica E, vol. 41, pp. 1127, 2009.

[38]V. T. Tran, J. P. Benoit and M. C. Venier Julienne, Int. J. Pharmaceut., vol. 407, pp. 1, 2011.

[39]T. Ioppolo, M. Kozhevnikov, V. Stepaniuk and V. Sheverev, Appl. Opt., vol. 47, pp. 3009, 2008.

[40]J. B. Jager, P. Noe, E. Picard, V. Calvo, E. Delamadeleine and E. Hadji, Physica E, vol. 41, pp. 1127, 2009.

[41]K. Miura, K. Tanaka and K. Hirao, J. Non Cryst. Solids, vol. 276, pp. 213-214, 1997.

[42]N. Kitamura, M. Makihara, M. Hamai, T. Sato, I. Mogi, S. Awaji, K. Watanabe and M. Motokawa, Jpn. J. Appl. Phys., vol. L324, pp. 39, 2000.

[43]N. Kitamura, M. Makihara, T. Sato, M. Hamai, I. Mogi, S. Awaji, K. Watanabe and M. Motokawa, J. Non-Cryst. Solids, vol. 624, pp. 293-295, 2001.

[44]I. Bica, Mater. Sci. Engin. B, vol. 77, pp. 210, 2000.

[45]L. Collot, V. Lefevre-Seguin, B. Brune, J. Raimond and S. Haroche, Europhys. Lett., vol. 23, pp. 327, 1992.

[46]C. H. Dong, L. He, Y. F. Xiao, V. Gaddam, S. Ozdemir, H. C. Guo and L. Yang, Appl. Phys. Lett., vol. 94, pp. 231119, 2009.

[47]M. Brenci, R. Calzolai, F. Cosi, G. Nunzi Conti, S. Pelli and G. C. Righini, Proc. SPIE, vol. 6158, pp. 61580, 2006.

[48]S. Arnold, S. Shopova and S. Holler, Opt. Express, vol. 18, pp. 281, 2010.

[49]S. Boriskina and L. Dal Negro, Opt. Lett., vol. 35, pp. 2496, 2005.

[50]F. Vollmer, D. Braun, A. Libchaber, M. Khoshsima, I. Teraoka and S. Arnold, Appl. Phys. Lett., vol. 80, pp. 4057, 2002.